

Molecular Weight Distributions in Free-Radical Polymerizations.

2. Low-Conversion Bulk Polymerization

Paul A. Clay and Robert G. Gilbert*

School of Chemistry, University of Sydney, New South Wales 2006, Australia

Gregory T. Russell

Department of Chemistry, University of Canterbury, Private Bag 4800, Christchurch, New Zealand

Received March 11, 1996; Revised Manuscript Received January 21, 1997[®]

ABSTRACT: Results are reported for the low-conversion bulk polymerizations of methyl methacrylate (up to 15% conversion) and styrene (up to 8%) at 50 °C with AIBN as the initiator. The rates were measured gravimetrically, and the time evolution of the full molecular weight distributions (MWDs) were measured by GPC. For both monomers, the rates obeyed $[AIBN]^{0.5 \pm 0.05}$, independent of conversion. MWD data were analyzed as $\ln P(M)$, where $P(M)$ is the pseudoinstantaneous number distribution; approximate analytic solutions for the MWD suggest that plots of $\ln P(M)$ vs M should show extensive linear regions if chain stoppage is by transfer, disproportionation, and/or chain-length-dependent termination. The cumulative number distribution is approximately the GPC distribution divided by the square of the molecular weight; pseudoinstantaneous number distributions were obtained by subtracting the appropriately normalized cumulative distributions at successive conversions. All MWD data show $\ln P(M)$ is linear in M for higher M , with the slope of this region being independent of conversion but increasing significantly with increasing $[AIBN]$. The combined MWD and rate data for styrene are consistent with chain stoppage being both by transfer to monomer and by termination (by combination) between long and short chains, long–long termination being too slow to be important; parameter values reproducing both the rate and the MWD involve both chain-length-dependent and chain-length-independent events, with the critical distance of interaction for termination being significantly greater than that of a monomer unit (as distinct from what is seen at intermediate conversion). For MMA, where termination is dominated by disproportionation, the rate and MWD data are best fitted by assuming that center-of-mass (chain-length-dependent) termination is at most only weakly rate-determining. Attempts to use the low- M shape of plots of $\ln P(M)$ to indicate whether termination occurs by combination or disproportionation were inconclusive.

1. Introduction

In a previous paper,¹ means were developed to calculate the molecular weight distribution (MWD) in free-radical polymerization (in the absence of branching and cross-linking) by both exact numerical means and by approximate analytic solutions. The approximate analytic solutions suggest important qualitative features of the MWD and relate these features to the appropriate rate coefficients. In this paper, we report an extensive series of experimental studies of rates and molecular weight distributions and compare these with theory. A major aspect of the theory is that it takes into account the dependence of the termination rate coefficient on the lengths of the two terminating chains, an effect first discussed long ago.^{2,3} In principle, our model^{1,4–9} gives MWDs for linear polymers solely from the rate coefficients for propagation and transfer and from the dependences of the diffusion coefficients of small species on their degree of polymerization and on the weight-fraction of polymer.

This paper examines the MWDs in low-conversion bulk free-radical polymerizations. Our primary aim is to test how our model¹ describes low-conversion bulk systems; a subsidiary aim is to see if such MWD data can quantify the relative amounts of combination and disproportionation. At low weight fractions of polymer (low conversion), (a) the termination rates and rate coefficients are highest, thereby minimizing the effect of competing chain-stoppage mechanisms such as trans-

fer, and (b) the rate of polymerization is approximately constant and, hence, the instantaneous and cumulative MWDs should be similar. In practice, as long as the polymerization is not allowed to proceed beyond a few percent conversion, one should obtain a “pseudoinstantaneous” MWD¹⁰ with relative ease, facilitating comparison with theory. A later paper¹¹ examines MWD data at higher conversion.

2. Theoretical Background

We summarize here our previous paper¹ as it applies to bulk polymerizations. Since here we consider only polymerizations at low weight-fractions of polymer, when the center-of-mass diffusion coefficients are large, it is possible to neglect reaction-diffusion (i.e., the diffusion of a radical chain-end due to propagation¹²). We also give an improved dependence of polymeric diffusion coefficients on the degree of polymerization.

The polymeric *radical* chain length distribution is needed to predict the (dead-chain) MWD. In a bulk polymerization, the population balance equations for radicals are (e.g., refs 9 and 13)

$$\frac{dR_1}{dt} = 2fk_d[I] + k_{tr}[M] \sum_{j=2}^{\infty} R_j - k_p^1[M]R_1 - 2R_1 \sum_{j=1}^{\infty} k_t^{1j} R_j \quad (1)$$

* Author for correspondence and proofs.

[®] Abstract published in *Advance ACS Abstracts*, March 1, 1997.

$$\frac{dR_i}{dt} = k_p^{i-1}[M]R_{i-1} - k_p^i[M]R_i - k_{tr}[M]R_i - 2R_i \sum_{j=1}^{\infty} k_t^{ij}R_j \quad i > 1 \quad (2)$$

where f = initiator efficiency, k_d = rate coefficient for initiator decomposition, I is the initiator, k_{tr} = rate coefficient for transfer to monomer (transfer to the chain-transfer agent is readily included, although transfer to the polymer and cross-linking require a more complex treatment), M is the monomer, R_i = concentration of radicals of degree of polymerization i , k_p^i = propagation rate coefficient of a radical containing i monomer units, and k_t^{ij} = bimolecular termination rate coefficient for termination between two radicals of degrees of polymerization i and j , respectively. Since eqs 1 and 2 are for radical species only, it is not necessary to distinguish between combination and disproportionation, because both result in the loss of two radicals (although the termination mode is required for the MWD). Steady-state solution of eqs 1 and 2 leads, in terms of a continuous degree of polymerization variable N , to an expression for $R(N)$, the concentration of radicals of degree of polymerization N . To specify $k_t(N, N')$, the continuous equivalent of k_t^{ij} , at low conversion, one notes that termination involves³ (a) the centers of mass of the two radicals diffusing into proximity (by center-of-mass diffusion of the radicals as a whole); (b) the radical centers themselves diffusing to the critical distance for reaction ("segmental diffusion"); and (c) the "chemical" barrier to reaction being overcome. Hence,

$$\frac{1}{k_t(N, N')} = \frac{1}{2\pi p(N, N')(D(N) + D(N'))\sigma N_A} + \frac{1}{k_t^0} \quad (3)$$

The first term of the right-hand side of eq 3 is step a: $p(N, N')$ is the spin factor (radicals must have opposite spin to terminate, and one has $1/4 \leq p \leq 1$; opposite spins form a singlet state, parallel spins form the triply-degenerate triplet, and hence, there is a one in four chance of opposite spins), σ is the critical separation of radical ends at which termination is always supposed to occur, and $D(N)$ is the center-of-mass diffusion coefficient of a radical of degree of polymerization N , with the overall mutual diffusion coefficient for the center-of-mass diffusion process being taken as the sum of the individual diffusion coefficients for each chain. The second term is a crude attempt to allow for steps b and/or c. A chain-length-independent k_t^0 may correspond^{14,15} to a segmental diffusion contribution to $k_t(N, N')$ or a rate coefficient for step c. Note that if k_t^0 has a finite value (i.e., if this term is significant in determining the MWD), then the numerical solution of the steady-state form of eqs 1 and 2 requires a complete iterative solution of these nonlinear equations, rather than the more rapid method that can be used if $k_t(N, N')$ is separable into terms involving N and N' .¹ The instantaneous number of dead polymer chains of degree of polymerization N , $P(N)$, is given by

$$P(N) = \frac{\partial \bar{P}(N)}{\partial t} = k_{tr}[M]R(N) + \int_1^{N-1} k_{tc}(N, N-N')R(N')R(N-N')dN + 2R(N) \int_1^{\infty} k_{td}(N, N')R(N')dN \quad (4)$$

where the subscripts d and c denote disproportionation and combination and the cumulative number MWD is denoted $\bar{P}(N)$. If the k_t^0 term in eq 3 is neglected and it is assumed that $p(N, N') = p$ is independent of both N and N' , then,¹

$$\lim_{N \rightarrow \infty} \left(\frac{\ln P(N)}{N} \right) = - \left(\frac{k_{tr}[M] + \langle k_t \rangle [R]}{k_p[M]} \right) \quad (5)$$

where $[R] = \int R(N) dN$ = total radical concentration and $\langle k_t \rangle$ = average termination rate coefficient:

$$\langle k_t \rangle = \int_1^{\infty} \int_1^{\infty} k_t(N', N) \frac{R(N)}{[R]} \frac{R(N')}{[R]} dN dN' \quad (6)$$

Equation 5 implies that, if the termination rate coefficient depends significantly on chain length, then the number MWD will be a single exponential at a high degree of polymerization. Disproportionation results in upward curvature of the distribution at low N , whereas for combination, the curvature is downward at low N . As noted,¹ it might prove possible to use this behavior experimentally to give information on the mode of termination. If termination is by both combination and disproportionation, then any concavity will be reduced. If k_t^{ij} is independent of chain length, the MWD for combination is much more concave down (extensive predicted $P(N)$ values have been presented previously;¹ some predicted MWDs are shown later in Figure 10).

2.1. Parameter Values Used in the Simulations.

The parameter values used in the simulations are usually the same as or close to those used previously,¹ except where more reliable values have come to light. Unless otherwise stated, all data are for the experimental temperature of 50 °C. For MMA, k_p ($\text{dm}^3 \text{mol}^{-1} \text{s}^{-1}$) = 615^{16,17} and 250 for styrene.^{18,19} Based on theory²⁰ and experiment,²¹ it is expected that for the very lowest degrees of polymerization, k_p^i will be greater than the long-chain value; for styrene, we employed $k_p^1 = 4k_p$, and for MMA, $k_p^1 = 5k_p$ and $k_p^2 = 2k_p$, all other k_p being assigned the long-chain value. The value of k_{tr} used was $9.0 \times 10^{-3} \text{ dm}^3 \text{mol}^{-1} \text{s}^{-1}$ for styrene²² and $3.5 \times 10^{-2} \text{ dm}^3 \text{mol}^{-1} \text{s}^{-1}$ for MMA;²³ the uncertainty in these quantities suggests that some latitude is possible in the choice of values used. For AIBN, k_d is²⁴ $9.7 \times 10^{-7} \text{ s}^{-1}$ in the presence of MMA and $2.97 \times 10^{-6} \text{ s}^{-1}$ in the presence of styrene. The initiator efficiency for AIBN was taken as²⁵ $f = 0.72$ for MMA and 0.6 for styrene. The value of k_t^0 was varied between 10^7 and $10^8 \text{ dm}^3 \text{mol}^{-1} \text{s}^{-1}$; the values used in the comparisons between model and experiment are those which gave the best accord with both rate and MWD data. The spin probability parameter, p , has been found to be $1/4$ for small radicals;²⁶ values between $1/4$ and $1/2$ are used here (values close to this can reproduce termination-dominated kinetics at higher conversion⁴). There is evidence²⁷ that segmental diffusion may be insignificant at low conversion termination in styrene; this suggests that one can use the size of a monomer unit, as opposed to coil size or the size of a dangling chain end, as the distance of interaction for step a for styrene; however, this may not be the case in general, and one can postulate greater encounter radii; e.g., the coil size may be applicable. The "expected" values of σ are 6.02 Å for polystyrene radicals⁹ and 5.9 Å for poly(MMA) radicals.²⁸

We next specify the dependence of the diffusion coefficients on radical length and weight fraction of

polymer, w_p . Extensive data on the diffusion of oligomeric species (up to $N = 10$) above c^* can be fitted by^{29,30}

$$D_f(w_p) = \frac{D_{\text{mon}}(w_p)}{I^\alpha} \quad \alpha(w_p) = 0.758 + 1.5 w_p \quad (7)$$

$D_{\text{mon}}(w_p)$ for solvent/polystyrene systems at 50 °C is taken as

$$\log(D_{\text{mon}}/\text{cm}^2 \text{ s}^{-1}) = -4.5018 - 0.42414 w_p - 8.5097 w_p^2 + 29.624 w_p^3 - 46.223 w_p^4 + 22.889 w_p^5 \quad (8)$$

as fitted to data from a range of experimental data.^{31–36} Equation 8, which is only valid for $w_p < 0.8$, corrects for minor errors in refs 4 and 13). For MMA at 50 °C, the equivalent relationship (valid for $w_p < 0.8$) determined from a range of experimental data^{29,36–41} is¹³

$$\log(D_{\text{mon}}/\text{cm}^2 \text{ s}^{-1}) = -4.386 - 3.200 w_p + 9.049 w_p^2 - 12.079 w_p^3 \quad (9)$$

3. Experimental Methods

A number of factors were considered when designing the experimental part of this work. A low w_p and relatively high initiator concentrations ensure that termination, rather than transfer, should be the dominant chain-stopping mechanism. Conversions were determined gravimetrically, whence rates were obtained (although there are more accurate methods for rate measurement). The reaction mixture was split into a number of vials and each vial treated as a separate sample, stopping the polymerization in the vials after varying the amounts of time. These samples were then used for gravimetry and the determination of the MWD. This method relies upon the assumption that the conditions will be identical in each of the separate vials containing the same reaction mixture. To ensure that the conditions in each of these separate vials were as close to each other as possible, stock solutions were prepared containing monomer and the required amount of initiator, and all samples with the same initiator concentration were prepared with this stock solution. In addition, the deoxygenation procedure was identical for each of the vials; i.e., the same gas (N_2), flow rate, and degassing time were used.

3.1. The Work of Balke and Hamielec. The conditions used here were based in part upon those used by Balke and Hamielec⁴² (B&H), who conducted the seminal and pioneering work in this field: an extensive investigation of the AIBN-initiated polymerization of MMA, right through to limiting conversion, at 50–90 °C. Note two features of their results at 50 °C: (i) the rate of polymerization was approximately constant up to a conversion of about 20% (B&H Figure 2), and (ii) the average cumulative molecular weights remained approximately constant over the same conversion range (B&H Tables XII, XIII, and XIV); no MWDs were presented for the polymerizations conducted at 50 °C. The work of B&H provides checks of the experimental procedures used in the present work. Of particular importance is the fact that the same conversion–time relationships were obtained under the same conditions. The present study uses a wider range of initiator concentrations than B&H, examines styrene as well as MMA, and focuses solely on low conversion.

The main difference between this work and that of B&H is one of approach. It is common practice to compare theory and experiment by seeing if accord can be obtained between “gross” observables such as the overall rate and $\langle M_n \rangle$ with physically reasonable values of requisite rate parameters. For example, B&H fitted their MWDs (actually, chromatograms in the form $G(V_e)$, i.e., concentration-sensitive detector response as a function of elution volume) with a single-parameter model, that parameter being the ratio of the pseudo-first-order rate

coefficient for disproportionation to that for propagation. Transfer was taken as negligible (over the whole conversion range), and classical kinetics were assumed, i.e., no chain-length dependence of the rate coefficients was allowed. Instantaneous MWDs were all found to have polydispersities close to 2.0, which was taken to mean that termination by combination could be ignored. However, such polydispersities can also be explained by (i) transfer control of the MWD (and certainly it would now seem that transfer to monomer does at least play some role in intermediate- and high-conversion MMA polymerizations²³), (ii) some chain-length-dependent termination by combination,^{43–45} and (iii) chain-length-independent disproportionation. This illustrates that accord between model and experiment alone is not sufficient for unambiguous microscopic understanding of polymerization kinetics.

The present approach is to obtain as much mechanistic information from the data before resorting to modeling. For example, the above theory shows that if termination depends on chain length, then $\ln P(M)$ should show an extensive linear region at higher molecular weights, and the slope of this linear region should vary in particular ways with conversion and initiator concentration. Comparing such *semiquantitative* predictions with experiment provides a means of *refuting* the assumptions inherent in the theory. Moreover, portions of a $\ln P(M)$ plot that are nonlinear might also provide qualitative mechanistic information. A quantitative comparison of data with theory, now in such forms as theoretical and observed values of (i) the slope of any linear region of a $\ln P(M)$ plot and (ii) the behavior of nonlinear regions, then provides a second step in the testing which can be seen as fine-tuning.

Since theory indicates that mechanistic information is most readily obtained from $\ln P(M)$, this is the form of our MWDs which we analyze.

3.2. Experimental Procedures. Four separate sets of experiments were conducted—two sets each for styrene and MMA. The variables within each set of experiments were initiator concentration and reaction time. Each of the two sets with the same monomer was performed under identical conditions except that, in the case of one of the MMA polymerization sets, a more stringent purification procedure was used. The initiator concentrations used were 0.1, 0.3, 0.5, and 1.0% by weight. These correspond to molar concentrations of 5.54×10^{-3} , 1.66×10^{-2} , 2.77×10^{-2} , and 5.54×10^{-2} mol dm^{-3} for MMA and 5.35×10^{-3} , 1.60×10^{-2} , 2.67×10^{-2} , and 5.35×10^{-2} mol dm^{-3} for styrene.

PCLC1. AIBN (2,2'-azobis(isobutyronitrile), Wako) was recrystallized from ethanol at 45 °C. MMA (BDH Ltd.) was washed twice with a 5% aqueous solution of NaOH to remove quinol, used as an inhibitor. The resulting monomer solution was washed twice with distilled water and dried over MgSO_4 followed by CaH_2 . Pure monomer was then obtained by fractional distillation under nitrogen at reduced pressure. Stock solutions of AIBN in MMA were prepared and then separated into 9-mm inner-diameter cylindrical glass vials sealed with rubber septa. The volume of solution in each vial was approximately 1 mL. The vials were kept on ice until needed. N_2 was bubbled through each solution—by use of a syringe passed through the septum—for 2 min prior to immersion in a water bath kept at a temperature of 50.0 ± 0.1 °C. After a specified length of time, each vial was removed from the water bath and 25 μL of a 10% solution of 2,6-di-*tert*-butylphenol in tetrahydrofuran (THF) was injected through the septum to quench polymerization. The sample was then transferred to a centrifuge tube and weighed. Methanol was added to precipitate the polymer, which was recovered by centrifuging and drying in a vacuum oven, and then weighed.

PCLC4. The procedure was exactly as for PCLC1 except that distillation under reduced pressure was the only purification of monomer as supplied. Also, after injection of inhibitor to quench polymerization, samples were simply transferred to an aluminum pan, and monomer was removed by drying overnight in an oven at approximately 60 °C. Following this removal of monomer, the resulting polymer was again weighed.

For **PCLC2** and **PCLC3**, the procedure was exactly as for PCLC4 except that styrene (Ajax) was used as monomer. The

differences in the experimental procedure between experiment sets PCLC1 and PCLC4, both of which used MMA, were the more stringent monomer purification in PCLC1 and the different methods for isolation of polymer. Preliminary experiments had suggested that the more stringent purification procedure was unnecessary, and the differing procedures were performed as a test of this hypothesis.

To verify that polymerization did not occur either before the vials were placed in the water bath or after addition of the quencher, samples of each stock solution were placed in identical vials and treated in an identical manner to all other samples, except that they were not placed in the water bath; i.e., each stock solution was quenched immediately after having N_2 bubbled through it and its conversion determined by gravimetry. In all cases, no polymer was recovered.

Since all polymerizations were quenched prior to the onset of the gel effect, the necessity of good heat transfer was not as critical as in the experiments of B&H.⁴² Although the sample vials used in this work had a slightly larger diameter than the ampules used by B&H, our vials should still have provided a large enough surface-to-volume ratio to ensure effective heat transfer. Another point is that a low volume of starting solution, ca. 1 cm³, was used so as to minimize the time required to heat the solution from 0 to 50 °C; negligible polymerization should have occurred during this heat-up period.

3.3. Gel Permeation Chromatography. A detailed examination of the molecular weight distributions is central to this work, so special care was taken in their measurement, especially since the successive subtraction needed to obtain pseudoinstantaneous distributions inherently leads to large uncertainty.

The GPC system used in this work included a Waters 510 HPLC pump operating at 0.6 mL/min. The pump output was directed through a section of large diameter tubing (1 mm) followed by a section of small diameter tubing (0.2 mm) to reduce pressure fluctuations caused by crossover of the pump heads. A Waters WISP 710B automated injection system was employed. All injection volumes were 100 μ L. Separation was performed on a single Waters Ultrastaygel linear 7-m column. Over the course of measurements conducted for this work, the plate count was $(10.2 \pm 0.4) \times 10^3$, which compares well with the manufacturer's value of 10.0×10^3 . For the detection of polystyrene, a Waters Model 441 UV absorbance detector operating at 254 nm was used. For the detection of PMMA, either a Waters R401 differential refractometer or an Erma Optical Works ERC-7510 RI detector was used. The temperature of the latter detector was kept constant at 35 °C. Data were collected by a Waters System interface module and Millennium 2010 V2.00 software.

Fourteen narrow MWD PS calibration standards (six supplied by Polymer Labs and eight by Waters) were used, covering a range of peak molecular weights from 2.9×10^3 to 1.02×10^7 . Standards were dissolved in THF. The concentration of standard solutions was kept below 0.02 wt %. For the two highest molecular weight standards (1.02×10^7 and 6.85×10^6), the concentration was kept below 0.01% to avoid chain shearing. It was also found that the presence of particulate matter in the precolumn guard filter, rough handling, and time contributed to peak degradation in the higher molecular weight calibration standards. To counteract peak degradation, the precolumn guard filter was cleaned regularly. Also, standard solutions were never shaken or stirred to promote dissolution of the polystyrene standards but rather were allowed to stand overnight for complete dissolution to occur. In general, the standard solutions were used within 48 h of their preparation and in the case of the two highest molecular weight standards within 24 h. Occasional problems were experienced with calibration drift, i.e., elution times of the same standards changing over the course of a complete set of GPC injections. To ensure that this did not affect the results, the GPC system was calibrated daily, and the absence of drift was ensured by injection of the same standard solution as the initial and final injection in each set of samples and standards.

For the case of PMMA, universal calibration⁴⁶ was used. The values of the Mark–Houwink parameters used were $K =$

$11.0 \times 10^{-6} \text{ dm}^3 \text{ g}^{-1}$ and $a = 0.725$ for PS²⁴ and $K = 7.5 \times 10^{-6} \text{ dm}^3 \text{ g}^{-1}$ and $a = 0.75$ for PMMA.²⁴ (The values of K given here are not in the standard units of mL g⁻¹; this has been done to draw attention to a bug in the Millennium 2010 V2.00 software that truncates the high molecular weight end of the MWD during the universal calibration procedure if the value of K is given in the standard units. The use of K in units of dm³ g⁻¹ provides a satisfactory workaround for this bug.)

The cumulative number MWD, $\bar{P}(M)$, or the cumulative weight MWD, $\bar{W}(M)$, are found from the GPC trace, $G(V_{el})$, through the relationships^{1,47}

$$\bar{P}(M(V)) = A \frac{\bar{W}(M)}{M} = A \frac{G(V_{el})}{M \frac{dM}{dV}} \quad (10)$$

A is an arbitrary constant and $V(M)$ is the calibration curve, i.e., the volume at which a monodisperse standard is eluted. For a linear calibration curve (i.e., $V(M) = a + b \log M$), one has^{1,47}

$$\bar{P}(M) = (\text{constant}) G(V_{el})/M^2 \quad (11)$$

The Millennium software performs the calibration procedure for an arbitrary calibration curve using eq 10 and outputs a distribution labeled "dwt/d(logM)", which we confirmed to be the cumulative logarithmic weight distribution $\bar{W}(\log M) = \bar{W}(M)M \ln 10$. The accuracy of an experimental MWD is limited *inter alia* by the accuracy of the calibration procedure. In this work, much care was taken to ensure that the GPC was accurately calibrated, including a nonlinear calibration curve— $\log M$, a cubic polynomial in V_{el} —being used in eq 10. This should help in making the low and high molecular weight ends of the experimental MWDs as accurate as possible, which is obviously important given the aims of this work.

4. Results

The results of sets PCLC1 and PCLC4 suggest that the more rigorous purification and isolation methods used in PCLC1 give no significant differences.

4.1. Conversion–Time Data and Rate of Polymerization. Conversion–time data for the duplicate MMA polymerizations (PCLC1 and PCLC4) agree acceptably, even though the monomer purification and polymer isolation procedures differed. Further, these data are in accord with those of B&H,⁴² where comparison is possible. Conversion–time data for the two duplicate sets of styrene polymerizations (PCLC2 and PCLC3) also show acceptable reproducibility.

The results for conversion, x , vs time, t , were used to find the rate of fractional conversion, dx/dt . While our data certainly indicate that dx/dt is approximately constant over the measured conversion ranges, our measurements were not frequent enough to have been able to detect any fine variations in dx/dt with conversion. For bulk systems, the polymerization rate $R_p = -d[M]/dt$ is given by

$$R_p = \frac{dx}{dt} [M]_0 (1 + \epsilon) \quad (12)$$

Here $\epsilon = (d_M - d_p)/d_p$, d_M and d_p being the densities of the monomer and polymer, respectively (finer corrections^{6,48} for density differences are deemed unnecessary).

Figure 1 shows R_p as a function of initiator (AIBN) concentration. The data fit $R_p \sim [I]^{0.52 \pm 0.04}$ for MMA and $R_p \sim [I]^{0.49 \pm 0.02}$ for styrene. These results are consistent with the 'classical' (chain-length-independent kinetics) relation $R_p \sim [I]^{0.5}$. If termination is allowed to depend upon chain length, then^{6,45,49} $R_p \sim [I]^y$, where $y < 0.5$,

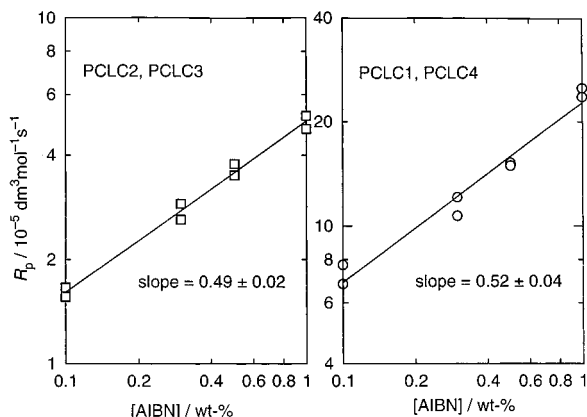


Figure 1. Variation of the rate of polymerization, R_p , with initiator concentration for the low-conversion polymerizations of styrene (PCLC2 and PCLC3) and MMA (PCLC1 and PCLC4).

and the stronger the dependence of termination is on chain length, the further y is from 0.5. For example, if the diffusion scaling exponent $\alpha(N) = 0.5$ (i.e., $k_t^{ij} \sim i^{-0.5}$ for all i) and there is no transfer, then $y = 0.33$, while $\alpha(N) = 0.6$ and no transfer results in $y = 0.29$. Introducing a finite k_t^0 (see eq 3) into the chain-length-dependent model gives a more classical variation of R_p with $[I]$.

Our rate data seem inconsistent with the suggestion that the k_t^{ij} which are rate-determining are chain-length dependent. A possible physical picture here is that if i is small and j is large, then k_t^{ij} might be roughly independent of i due to chain-end encounter being highly hindered;^{50,51} equally, termination might be slowed down and rendered chain-length-independent via some other mechanism. Nevertheless, there are several difficulties with the suggestion of chain-length-independent termination. First, this would predict that the molecular weight distribution for a combination-dominated system would have the form $P(M) \propto M \exp(-(\text{constant})M)$, which contradicts the observed $P(M)$ for styrene (it will be seen in Figures 5 and 6 that $\ln P(M)$ is quite linear), for which termination is overwhelmingly by combination.^{52,53} However, this argument cannot be used for MMA, where disproportionation dominates.^{54,55} Further, direct measurement²⁶ has shown that small radical termination rates in solution are always accurately given by the Smoluchowski equation with $p = 0.25$, so for styrene, one expects $k_t^{1,1} \approx 10^9 \text{ dm}^3 \text{ mol}^{-1} \text{ s}^{-1}$. If termination were chain-length-independent, one would therefore have to expect $\langle k_t \rangle \approx 10^9 \text{ dm}^3 \text{ mol}^{-1} \text{ s}^{-1}$, a value which is far too high to explain the observed rates and molecular weights. In fact, small radical studies²⁶ show that termination rate coefficients indeed scale with the mutual diffusion coefficient, which leads to the expectation that $k_t^{ij} \sim i^{-0.5}$ for small i at least. However while $k_t^{ij} \sim i^{-0.5}$ can explain⁵ the magnitude of experimental $\langle k_t \rangle$, there is still the difficulty of why the dependence of R_p on $[I]$ is not weaker than 0.5.

Another possible explanation is that chain stopping is transfer-determined. Under such circumstances, $R_p \sim [I]^{0.5}$ regardless of the chain-length-dependence of termination.⁶ While it is unlikely that transfer to monomer could be a dominant chain-stopping event in low-conversion polymerizations employing the concentrations of AIBN which were used, it is possible that an adventitious impurity may have acted as a chain transfer agent. However, a difficulty with this suggestion is that if chain stopping is determined by transfer,

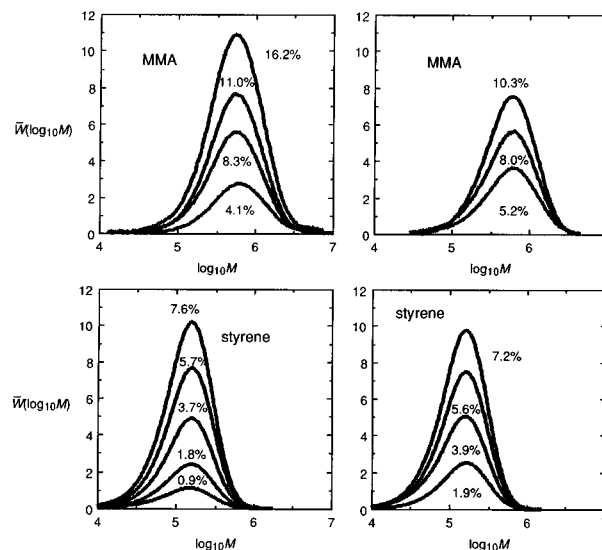


Figure 2. Typical cumulative MWDs plotted as $\bar{W}(\log M)$ vs $\log M$ for sets PCLC1 and PCLC4 (low-conversion bulk polymerization of MMA) and sets PCLC2 and PCLC3 (low-conversion bulk polymerization of styrene); in each case, the data are for 0.5 wt % AIBN and are for a range of conversions as indicated.

then so too is the MWD, and hence, one would expect the slope of $\ln P(M)$ vs M to be independent of $[I]$ (see eq 5). In fact, it will be seen that our data show a dependence of these slopes on $[I]$.

A third explanation for $R_p \sim [I]^{0.5}$ is as follows.^{6,56} If the rates of termination were determined by the rates of polymer self-diffusion, then $\langle k_t \rangle$ will decrease as the polymer concentrations increase over the low conversion regime. However, there is some evidence^{57,58} that in fact values of $\langle k_t \rangle$ can increase slightly over the low conversion regime, say until 5–10% conversion is reached. There is some debate as to the exact physical reason for this increase⁵⁹ (quite subtle effects might be involved, such as hydrodynamic interaction between chains,⁶⁰ which will diminish with increasing w_p), but it would seem accepted that the longer the terminating chains, the greater the extent to which k_t^{ij} increases over this initial conversion regime.⁵⁹ The latter thus explains why experiments⁵⁷ have found that the lower $[I]$ is, the greater this initial increase of $\langle k_t \rangle$ is (with lower $[I]$, there are more long chains). The termination parameters of section 2.1 (which give a description of how self-diffusion coefficients vary with conversion) do not incorporate such subtle phenomena. However, if this effect is real, then it must result in the increase of $\langle k_t \rangle$, with $[I]$ being stronger at zero conversion than at, say, 5% conversion, which is not observed: there is no evidence of any significant downward curvature—consistent with a noticeably increasing $\langle k_t \rangle$ —in any of our $x(t)$ data.

A fourth possibility is that the critical interaction distance for termination (σ) might be much greater than the size of a monomer unit, and indeed, simulations with a large σ , taken together with a finite value of k_t^0 , also give an exponent y closer to 0.5.

Given the above discussion, it would seem justified to conclude that in MMA and styrene polymerizations at least, the variation of the average low conversion rates with $[I]$ presently defies unambiguous microscopic understanding.

4.2. Molecular Weight Distributions. Figure 2 shows some typical cumulative MWDs for the four sets of experiments; the MWDs are presented as $\bar{W}(\log M)$, in essence, how MWDs are yielded by GPC. The MWDs

have been normalized and then scaled according to the percentage conversion of monomer into polymer at the time at which the samples were taken. When presented in this form, one can gain some idea of the evolution of the MWD with time or conversion. Pseudoinstantaneous MWDs are obtained by subtracting one conversion-normalized cumulative MWD from another (see eq 4):

$$W(\log M) \text{ between } x_1 \text{ and } x_2 = \bar{W}(\log M; x_2) - \bar{W}(\log M; x_1)$$

$$\int_0^\infty \bar{W}(\log M; x_i) d \log M = x_i \quad i = 1, 2 \quad (13)$$

For all the polymerizations conducted in this work, the MWDs have a similar monomodal shape. As the initiator concentration is increased, the MWD is shifted to lower molecular weights while at the same time retaining the same qualitative shape. This can be readily explained as a greater contribution of termination to chain stoppage at higher initiator concentrations, resulting in a lower average chain length. The MWD changes little as conversion increases up to values of 16% for one MMA polymerization and 8% for styrene polymerization. This indicates that the rate of chain stoppage is approximately constant over these conversion ranges for both of these systems.

In general, experimental average molecular weights were reproducible (sets PCLC1 and PCLC4 for MMA and PCLC2 and PCLC3 for styrene). The agreement between experiments is worst at the lowest initiator concentrations (for which the uncertainty in the initiator concentration is 5–7%) and best at higher initiator concentrations (for which the uncertainty in the initiator concentration is less than 1%). The difference in the uncertainty at different initiator concentrations may be a result of the use of constant amounts of monomer being used in the preparation of stock solutions rather than constant amounts of initiator.

The number MWD, plotted as $\ln P(M)$, might provide mechanistic information. If linearity of this plot at higher M is observed, this suggests that chain stoppage is dominated by transfer and/or chain-length-dependent termination. The long-chain slope of $\ln P(M)$ gives information about the rate of chain stoppage compared to propagation, while the short-chain portion of $\ln P(M)$ can give information about the mode of termination operative during the polymerization. Figures 3–6 show the MWD data of polymerizations PCLC1–4 as both $\ln \bar{P}(M)$ (cumulative number MWD) and $\ln P(M)$ (instantaneous number MWD). It is actually the instantaneous MWD which gives mechanistic information, but under conditions where the kinetics do not change much with time, then the instantaneous MWD will be well-approximated by the cumulative MWD, which thus can be used for mechanistic interpretation. The advantage of being able to use $\ln \bar{P}(M)$ for this purpose is that they are not nearly as noisy as $\ln P(M)$.

Figures 3–6 show that the slope of $\ln \bar{P}(M)$ becomes steeper (more negative) as the initiator concentration increases. The steeper $\ln \bar{P}(M)$ indicates that the rate of chain stoppage is increasing, as expected with increasing initiator concentration. This is consistent with average molecular weights becoming lower with increasing initiator concentration, as seen from our plots of $\bar{W}(\log M)$. Figures 3–6 also show that the MWD, when plotted as $\ln P(M)$, changes little in shape with conversion up to $x \approx 15\%$. This result is in keeping with both

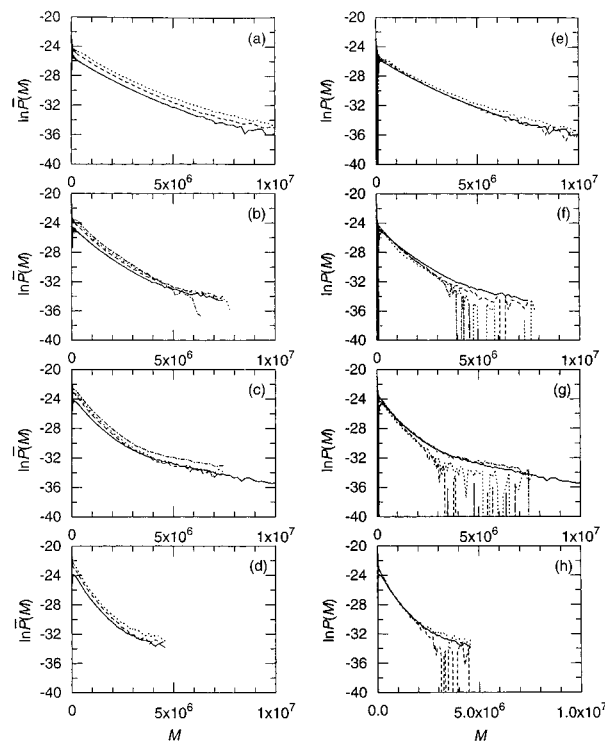


Figure 3. Number MWDs for set PCLC1 (low conversion bulk polymerization of MMA). a–d: Cumulative MWDs plotted as $\ln \bar{P}(M)$ vs M . All conversions in percent (a) $[AIBN] = 0.1$ wt %. Conversions: 2.7 (—), 5.9 (---), 9.7 (···). (b) $[AIBN] = 0.3$ wt %. Conversions: 3.2 (—), 6.5 (---), 8.7 (···), 11.6 (---). (c) $[AIBN] = 0.5$ wt %. Conversions: 4.1 (—), 8.3 (---), 11.0 (···), 16.2 (---). (d) $[AIBN] = 1.0$ wt %. Conversions: 3.1 (—), 7.1 (---), 11.2 (···). e–h: Instantaneous MWDs plotted as $\ln P(M)$ vs M . (e) $[AIBN] = 0.1$ wt %. Conversions: 0–2.7 (—), 2.7–5.9 (---), 5.9–9.7 (···). (f) $[AIBN] = 0.3$ wt %. Conversions: 0–3.2 (—), 3.2–6.5 (---), 6.5–8.7 (···), 8.7–11.6 (---). (g) $[AIBN] = 0.5$ wt %. Conversions: 0–4.1 (—), 4.1–8.3 (---), 8.3–11.0 (···), 11.0–16.2 (---). (h) $[AIBN] = 1.0$ wt %. Conversions: 0–3.1 (—), 3.1–7.1 (---), 7.1–11.2 (···).

the constancy of the $\bar{W}(\log M)$ over the conversion range studied and the approximately constant rate of polymerization, all evidence that the rate of chain stoppage is approximately constant over the first 10–15% of conversion.

One unexpected feature of the cumulative MWDs presented in Figures 3–6 is the curvature in the high molecular weight portion of some, but not all, of the distributions: e.g., in panels c and d of Figure 3. Figure 2 shows that the point at which the curvature in $\ln \bar{P}(M)$ occurs is on the high molecular weight tail of the MWD. The extent of curvature is not consistent for experiments under the same conditions, as shown in panels c of Figures 3 and 4. The origin of this curvature will be discussed later.

Figures 3–6 also show pseudoinstantaneous MWDs in the form $\ln P(M)$ for the polymerizations PCLC1–4. Because the cumulative MWDs change little with conversion, it is expected that the instantaneous MWD should (for low conversion!) essentially be the same as the cumulative MWD. As can be seen from Figures 3–6, this is indeed the case, except for the high and low molecular weight portions of the instantaneous MWDs, which are quite noisy and/or subject to large uncertainty. These regions in which $\ln P(M)$ is noisy stem from those parts of the MWD which correspond to low detector response in the GPC: the low and high molecular weight tails. The subtraction of two small signals results in a great increase in noise and/or uncertainty

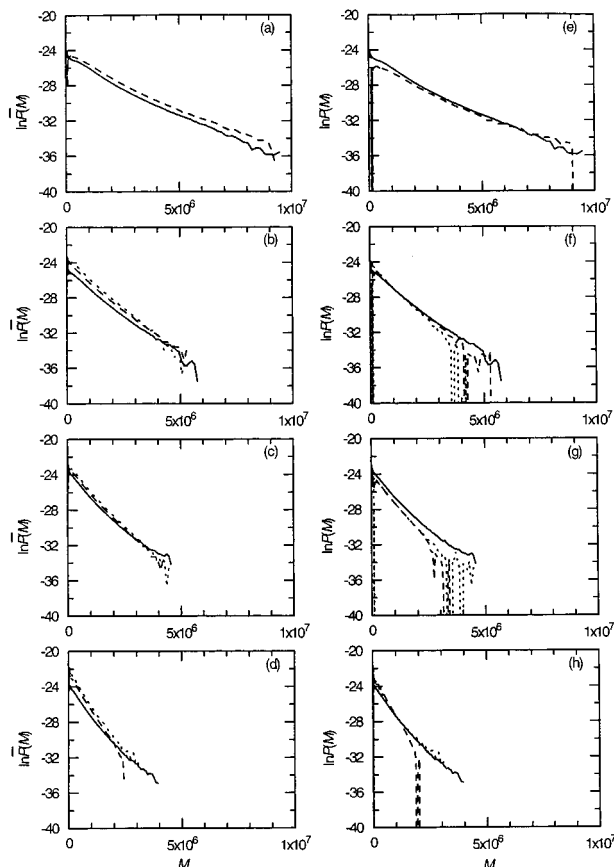


Figure 4. Number MWDs for set PCLC4 (low conversion bulk polymerization of MMA) a–d: Cumulative MWDs plotted as $\ln P(M)$ versus M . All conversions in percent. (a) $[AIBN] = 0.1$ wt %. Conversions: 7.09 (—), 11.22 (---). (b) $[AIBN] = 0.3$ wt %. Conversions: 2.85 (—), 6.12 (---), 9.06 (···). (c) $[AIBN] = 0.5$ wt %. Conversions: 5.24 (—), 7.97 (---), 10.34 (···). (d) $[AIBN] = 1.0$ wt %. Conversions: 2.77 (—), 7.45 (---), 11.37 (···). e–h: Instantaneous MWDs plotted as $\ln P(M)$ vs M . (e) $[AIBN] = 0.1$ wt %. Conversions: 0–7.09 (—), 7.09–11.22 (---). (f) $[AIBN] = 0.3$ wt %. Conversions: 0–2.85 (—), 2.85–6.12 (---), 6.12–9.06 (---). (g) $[AIBN] = 0.5$ wt %. Conversions: 0–5.24 (—), 5.24–7.97 (---), 7.97–10.34 (---). (h) $[AIBN] = 1.0$ wt %. Conversions: 0–2.77 (—), 2.77–7.45 (---), 7.45–11.37 (---).

in the pseudoinstantaneous MWD. The onset of noise in the high molecular weight portion of the MWD corresponds to the point at which a change in slope occurs in some of the cumulative MWDs; hence, this curvature may be an artifact of the tail of the MWD.

The pseudoinstantaneous $\ln P(M)$ for styrene are essentially linear at high molecular weights, as predicted in eq 5. It is this result for styrene, where combination is the dominant termination mode, that shows that *chain-length-dependent termination must be a significant effect*. If termination by combination were independent of chain length, then one would have $P(M) \propto M \exp(-2M/\langle M_n \rangle)$ —see, e.g., ref 13. This chain-length-independent functional form has a distinct maximum at relatively high M on a $\ln P(M)$ plot (as illustrated later in Figure 10), and this is not seen experimentally.

Rewritten in terms of molecular weight rather than degree of polymerization, eq 5 becomes

$$\lim_{M \rightarrow \infty} \left(\frac{\ln P(M)}{M} \right) \equiv - \frac{\Lambda_{\text{pred}}}{M_0} \quad (14)$$

where M_0 is the molecular weight of the monomer unit. This defines the dimensionless quantity Λ_{pred} , which,

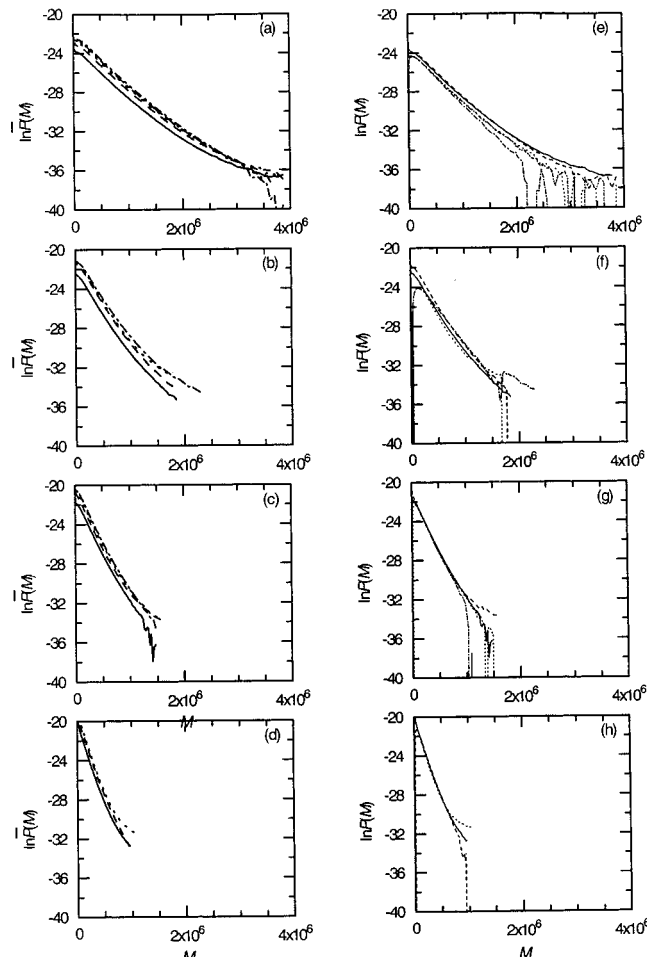


Figure 5. Number MWDs for set PCLC2 (low conversion bulk polymerization of styrene). a–d: Cumulative MWDs plotted as $\ln P(M)$ vs M . All conversions in percent. (a) $[AIBN] = 0.1$ wt %. Conversions: 0.34 (—), 1.20 (---), 2.08 (---), 2.84 (---). (b) $[AIBN] = 0.3$ wt %. Conversions: 0.53 (—), 1.30 (---), 2.78 (---), 4.37 (---), 5.63 (---). (c) $[AIBN] = 0.5$ wt %. Conversions: 0.90 (—), 1.84 (---), 3.69 (---), 5.68 (---), 7.59 (---). (d) $[AIBN] = 1.0$ wt %. Conversions: 3.21 (—), 5.63 (---). e–h: Instantaneous MWDs plotted as $\ln P(M)$ vs M . (e) $[AIBN] = 0.1$ wt %. Conversions: 0–0.34 (—), 0.34–1.20 (---), 1.20–2.08 (---), 2.08–2.84 (---). (f) $[AIBN] = 0.3$ wt %. Conversions: 0–0.53 (—), 0.53–1.30 (---), 1.30–2.78 (---), 2.78–4.37 (---), 4.37–5.63 (---). (g) $[AIBN] = 0.5$ wt %. Conversions: 0–0.90 (—), 0.90–1.84 (---), 1.84–3.69 (---), 3.69–5.68 (---), 5.68–7.59 (---). (h) $[AIBN] = 1.0$ wt %. Conversions: 0–3.21 (—), 3.21–5.63 (---).

for example, would be the transfer constant to monomer if this were the only chain-stopping event or more generally $(k_{tr}[M] + \langle k_t \rangle [R]) / k_p [M]$. One can compare the values of Λ_{pred} with the experimental values of Λ_{exp} obtained from MWDs through the relationship

$$\Lambda_{\text{exp}} = -M_0(\text{slope of linear region of } \ln P(M)) \quad (15)$$

The values of Λ_{exp} from the polymerizations of both styrene and MMA are shown in Figures 7 and 8. Figure 7 shows that Λ_{exp} does not change significantly with conversion, while Figure 8 shows that Λ_{exp} increases with increasing initiator concentration. Duplicate GPC runs for styrene (PCLC2 and PCLC3) show little variation in Λ_{exp} .

The range of molecular weights over which Λ_{exp} was determined must necessarily vary with initiator concentration and monomer. In general, the guidelines used were that the fit be performed over a range of

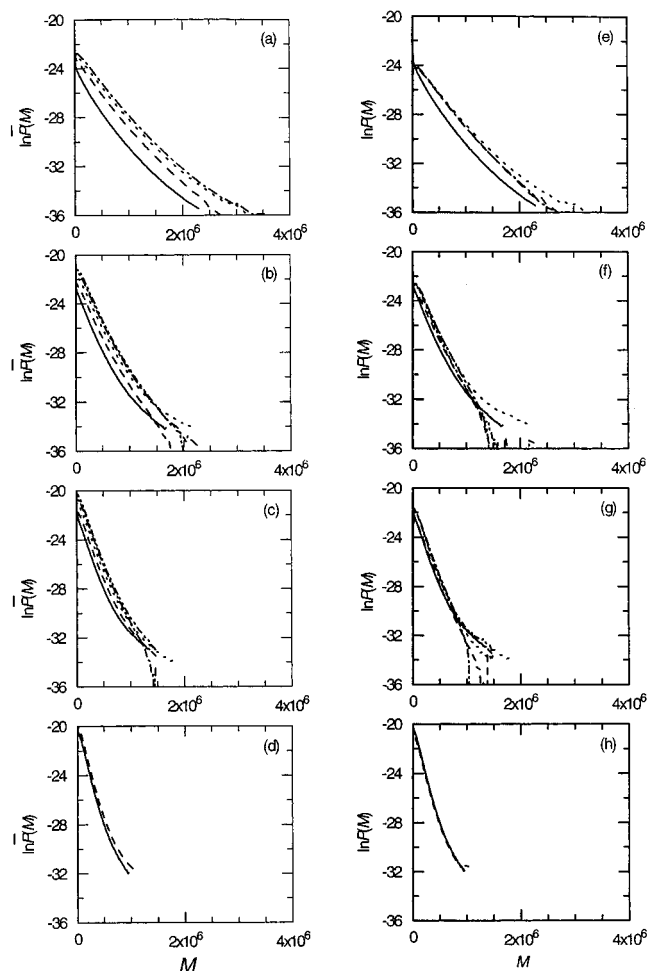


Figure 6. Number MWDs for set PCLC3 (low conversion bulk polymerization of styrene). a–d: Cumulative MWDs plotted as $\ln P(M)$ vs M . All conversions in percent. (a) $[AIBN] = 0.1$ wt %. Conversions: 1.15 (—), 2.45 (---), 3.24 (- - -), 3.95 (- · - ·), 4.73 (- · - ·). (b) $[AIBN] = 0.3$ wt %. Conversions: 1.45 (—), 4.40 (---), 5.71 (- - -), 6.67 (- · - ·). (c) $[AIBN] = 0.5$ wt %. Conversions: 1.88 (—), 3.91 (---), 5.56 (- - -), 7.24 (- · - ·). (d) $[AIBN] = 1.0$ wt %. Conversions: 2.87 (—), 5.23 (---), 8.11 (- - -). e–h: Instantaneous MWDs plotted as $\ln P(M)$ vs M . (e) $[AIBN] = 0.1$ wt %. Conversions: 0–1.15 (—), 1.15–2.45 (---), 2.45–3.24 (- - -), 3.24–3.95 (- · - ·), 3.95–4.73 (- · - ·). (f) $[AIBN] = 0.3$ wt %. Conversions: 0–1.45 (—), 1.45–4.40 (---), 4.40–5.71 (- - -), 5.71–6.67 (- · - ·). (g) $[AIBN] = 0.5$ wt %. Conversions: 0–1.88 (—), 1.88–3.91 (---), 3.91–5.56 (- - -), 5.56–7.24 (- · - ·). (h) $[AIBN] = 1.0$ wt %. Conversions: 0–2.87 (—), 2.87–5.23 (---), 5.23–8.11 (- - -).

molecular weights such that $\ln P(M)$ had as little noise as possible while the molecular weight was as large as possible. As an example, for the polymerizations of MMA at 0.1 wt % AIBN, Λ_{exp} was found from a linear fit of the slope of $\ln P(M)$ over the range from 1×10^6 to 6×10^6 .

Figures 7 and 8 compare Λ_{exp} and Λ_{pred} calculated with various models. The most noticeable difference between the predicted and experimental results is that the values of Λ_{exp} are essentially invariant with conversion (Figure 7), while the values of Λ_{pred} with $k_t^0 = \infty$ show a distinct decrease with increasing conversion. The reason for this predicted decrease is that the value of D_{mon} decreases with conversion, while the scaling exponent α (eq 7) increases with conversion. On both of these accounts, $\langle k_t \rangle$ decreases with conversion, unless these effects are overwhelmed by a finite k_t^0 . The experimental data in the form of Λ_{exp} lead to the inference that $\langle k_t \rangle$ is approximately constant over the

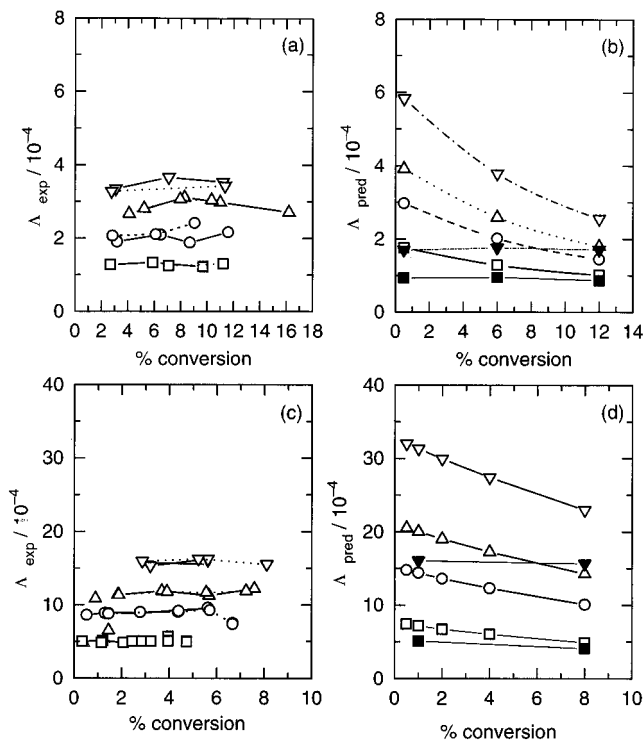


Figure 7. (a) Plot of Λ_{exp} as a function of percentage conversion for all MMA low-conversion data for 5.54×10^{-3} (\square), 1.66×10^{-2} (\circ), 2.77×10^{-2} (\triangle), and 5.54×10^{-2} (∇) mol dm^{-3} AIBN. (b) Plot of Λ_{pred} for the same conditions as in a, with $k_t^0 = \infty$ (open symbols) and $10^7 \text{ dm}^3 \text{ mol}^{-1} \text{ s}^{-1}$ at the lowest and highest $[AIBN]$ (filled symbols). (c) Plot of Λ_{exp} as a function of percentage conversion for all styrene low-conversion data for 5.35×10^{-3} (\square), 1.60×10^{-2} (\circ), 2.67×10^{-2} (\triangle), and 5.35×10^{-2} (∇) mol dm^{-3} AIBN. (d) Plot of Λ_{pred} as a function of percentage conversion for the same initiator concentrations shown in c, with $k_t^0 = \infty$ (open symbols) and $10^8 \text{ dm}^3 \text{ mol}^{-1} \text{ s}^{-1}$ at the lowest and highest $[AIBN]$ (filled symbols).

first 10–15% of conversion, and accord between Λ_{exp} and Λ_{pred} can be obtained by using the same (finite) values of k_t^0 which give accord with the observed behavior of the rate, as shown in the figures.

We turn now to considering the variation of Λ with $[I]$, shown in Figure 8. Equation 5 shows that if transfer is the sole chain-stopping event, then Λ will be independent of $[I]$. The fact that our Λ_{exp} increase with $[I]$ therefore proves that termination must be a significant chain-stopping event in our low-conversion polymerizations. Consider now the limit of termination being the only chain-stopping event. If termination is chain-length-independent, then $[R] \sim [I]^{0.5}$, so $\Lambda \sim [I]^{0.5}$ (see eq 5). However, if termination is chain-length-dependent, then both $\langle k_t \rangle$ and $[R]$ increase with $[I]$, although the $[R]$ dependence is now weaker than $[R] \sim [I]^{0.5}$. Nevertheless, simulation shows that $\langle k_t \rangle [R] \sim \Lambda$ has a stronger than 0.5 scaling with $[I]$ if there is chain-length dependence, and the stronger this dependence, the stronger this scaling: e.g., if $\alpha(N) = 0.5$ (i.e., $k_{ti} \sim i^{-0.5}$) and there is no transfer, then $\Lambda_{\text{pred}} \sim [I]^{0.67}$. The observation that $\Lambda_{\text{exp}} \sim [I]^{0.45 \pm 0.04}$ for MMA and $[I]^{0.50 \pm 0.01}$ for styrene suggests chain stoppage by chain-length-independent termination only or by both transfer and chain-length-dependent termination. MMA calculations with a relatively strong chain length dependence for termination (see section 2.1) give $\Lambda_{\text{pred}} \sim [I]^{0.47}$, almost exactly the experimental trend (see Figure 8). For styrene, the lower k_{tr} results in less predicted chain stoppage by transfer and so in stronger variation of Λ_{pred} with $[I]$, e.g., $\Lambda_{\text{pred}} \sim [I]^{0.67}$ at $x = 0.08$ (Figure 8).

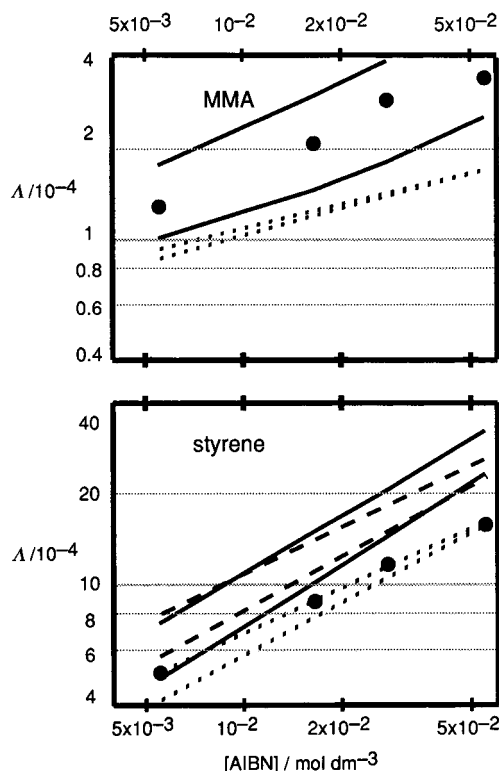


Figure 8. Dependence of Λ on [AIBN] for MMA and styrene as double-logarithmic plot. Points: experiment (the dependence on conversion is negligible); the data fit $\Lambda_{\text{exp}} \propto [\text{AIBN}]^{0.45 \pm 0.04}$ (MMA) and $[\text{AIBN}]^{0.50 \pm 0.01}$ (styrene). Lines: fit with various models at conversions = 0.5% (upper line of pair) and 12% (lower line of pair). (—) $k_t^0 = \infty$; (···) $k_t^0 = 10^7$ (MMA) and 10^8 (styrene) $\text{dm}^3 \text{mol}^{-1} \text{s}^{-1}$; (---) for styrene only, $k_t^0 = 10^8 \text{ dm}^3 \text{mol}^{-1} \text{s}^{-1}$, larger value of σ and other parameters as described in the text.

However, with minor changes, including a higher k_{tr} , a finite value of k_t^0 , and a larger value of the critical interaction distance σ , the variation of both Λ_{exp} and R_p with [I] and with conversion for styrene can be successfully simulated. A suitable parameter set is $p = 1/2$ (recall $1/4 \leq p \leq 1$), the interaction distance, σ , is 10 times that of a monomer unit (which can be interpreted as suggesting that a size such as that of a coil or dangling chain end rather than that of a monomer unit is the critical interaction distance at low conversion), $k_{\text{tr}} = 2 \times 10^{-2} \text{ dm}^3 \text{mol}^{-1} \text{s}^{-1}$ (a factor of 2 greater than the most accepted literature value²² but in accord with new measurements of the effective transfer constant under similar conditions¹¹), and $k_t^0 = 10^8 \text{ dm}^3 \text{mol}^{-1} \text{s}^{-1}$. This parameter set yields $R_p = 2.7 \times 10^{-4} [\text{I}]^{0.47}$ (units of $\text{mol dm}^3 \text{etc.}$), essentially independent of conversion over the range studied here and in accord with experiment ($R_p = 2.1 \times 10^{-4} [\text{I}]^{0.49}$). As discussed below and shown in Figure 10, these parameters also give acceptable accord with the experimental $\ln P(M)$.

Finally, consider the magnitude of the Λ_{pred} values. Referring to Figure 7, it is clear that for the MMA polymerizations, the values of Λ_{exp} and Λ_{pred} with $k_t^0 = \infty$ agree well in general and very well at $x = 0.06$. For MMA, a value of $k_t^0 = 10^7 \text{ dm}^3 \text{mol}^{-1} \text{s}^{-1}$ (which again makes the termination process more chain-length-independent) is needed to give a value of Λ which is approximately independent of conversion but (compared to $k_t^0 = \infty$) worsens the agreement with the dependence of Λ on [AIBN] as well as the absolute value of this quantity; this non-zero value of k_t^0 also improves the dependence of R_p on [AIBN] but worsens the absolute

value. For styrene, Λ_{pred} are generally too high for $k_t^0 = \infty$ and other "expected" values of parameters such as σ , especially at high [I] and the lowest conversions; however, using the alternative parameter values just discussed gives acceptable agreement with the observed dependence of Λ_{exp} on [AIBN], as shown in Figure 8. Thus, with styrene at low conversion, accord with the experimental dependence of both rate and high- M slope can be obtained by assuming that there are significant chain-length-dependent and -independent components to termination, with the critical interaction distance for termination being much greater than the size of a monomer unit.

4.3. Complete number MWDs. One motivation for examining MWDs was that the predicted differences are most marked between the MWD produced if all termination is either only by combination or only by disproportionation: the low- M portion of $\ln P(M)$ is concave down and up, respectively.

Experimental measures of the low- M MWDs involve several difficulties. (i) When product polymer is isolated by precipitation, some low molecular weight material can fail to precipitate out. It was for this reason that we mostly isolated polymer by evaporation only. However, even in the one set (PCLC1) where polymer was precipitated prior to drying, the low- M portions of the MWDs seem comparable to those of the duplicate (PCLC4). (ii) Two factors combine to produce poor sensitivity to low- M species: (a) the detectors used are sensitive to the mass of polymer and not the number of molecules present, and (b) the mass of polymer is measured as a function of elution volume, which is approximately proportional to $\ln M$. The combined result of these effects is that the GPC signal is approximately proportional to $M^2 P(M)$ (eq 11). Therefore, even though low- M chains may be the most numerous, the sensitivity to them is low, a problem which cannot be avoided if GPC is used. (iii) Finally, there is the possibility that (despite our purification procedures) our samples contained small amounts of impurities which may act as chain-transfer agents (such is not unlikely for both styrene⁶¹ and MMA⁶²) which may be rapidly consumed, even at the low conversions studied here. The effect of such impurities would be¹³ to produce an artifactual low- M upturn in $\ln P(M)$. One consequence of the low sensitivity of the GPC system to low- M species is that the subtraction technique used to determine pseudoinstantaneous distributions gives large uncertainties at low M . To circumvent this partly, MWDs of the samples taken at the lowest conversion (1–3%) should best approximate truly instantaneous MWDs.

Figure 9 shows $\ln \bar{P}(M)$ for the lowest conversion sample from each MMA experiment (i.e., a magnified view of parts of Figures 3 and 4); simulated instantaneous MWDs are also shown. Although the experimental $\ln \bar{P}(M)$ are for about 0–3% conversion, $x = 0.06$ was used in calculations because this was the value of x for which Λ_{pred} agreed best with Λ_{exp} for MMA. The simulations show that $P(M)$ becomes independent of the termination mode at high M and that not just the slope but also the nonlinear portions of our simulated $\ln P(M)$ agree with experiment for MMA; this quantitative agreement extends down to quite low M .

We now consider the question of the shape of the MWD at low M . In all cases the experimental distributions become noisy for $M \lesssim 2 \times 10^5$, which unfortunately is where the curvature differences of the predicted distributions are more pronounced. Nevertheless, all

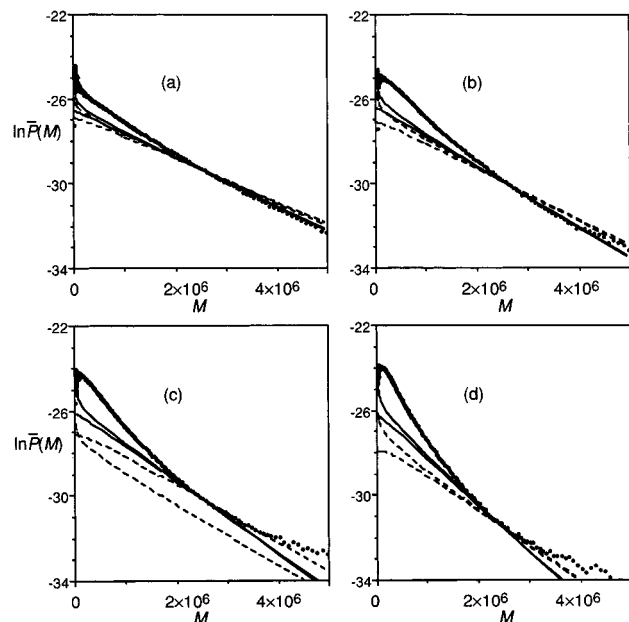


Figure 9. Simulated (broken lines, $k_t^0 = \infty$; full lines $k_t^0 = 10^7 \text{ dm}^3 \text{ mol}^{-1} \text{ s}^{-1}$) and experimental (heavy points) for lowest-conversion $\ln P(M)$ at (a) 5.54×10^{-3} , (b) 1.66×10^{-2} , (c) 2.77×10^{-2} , and (d) $5.54 \times 10^{-2} \text{ mol dm}^{-3}$ AIBN in set PCLC1 (MMA). The simulated MWDs are shown for all termination by disproportionation (concave up at low M), and for all termination by combination (concave down at low M), and for all simulated MWDs are for conditions at 6.0% conversion and for comparison purposes are normalized to have the same value as experiment at $M = 2.5 \times 10^6$.

data, except for the lowest [AIBN] in PCLC1 and the second highest [AIBN] in PCLC4, show good agreement with the predicted MWD obtained assuming all termination by combination. Even in those two cases in which agreement with the simulation assuming combination is not so good, the agreement with the simulations assuming disproportionation is no better. However, extensive investigations have always suggested that MMA termination tends to occur by disproportionation, e.g., from studies of small-radical termination reactions.²⁶ Most compelling of all such evidence is the recent use of MALDI-TOF mass spectroscopy for PMMA at 0 °C,⁵⁴ which showed the great majority of low- M chains to contain exactly one initiator-derived end group. Because usually (but not always!) the activation energy for disproportionation is greater than that for recombination,⁵³ increasing the temperature is expected to promote disproportionation over combination; thus, it is unclear how the 50 °C findings of the present $\ln P(M)$ data are to be understood. However, (a) the present data are reliable only for chains of much higher M than in the MALDI results, and (b) the possibility cannot be excluded of artifacts from both GPC (see below) and/or adventitious chain-transfer agent (see above) at these low molecular weights in our system.

We turn now to the low-conversion $\ln P(M)$ for styrene, given in Figure 10. In this case, (pseudo)-instantaneous distributions at ca. 2% are shown, since the very lowest conversion data may be contaminated by trace impurity effects, etc., which may be present at early times; these artifacts should be reduced by the subtraction used to give the pseudoinstantaneous $P(M)$. Some experimental distributions (e.g., Figure 10c) show a sharp upturn at low M . The apparent steep drop-off seen in Figure 10d at the lowest molecular weights is not seen in the duplicate experiments and must thus be an artifact due to baseline subtraction. However, the

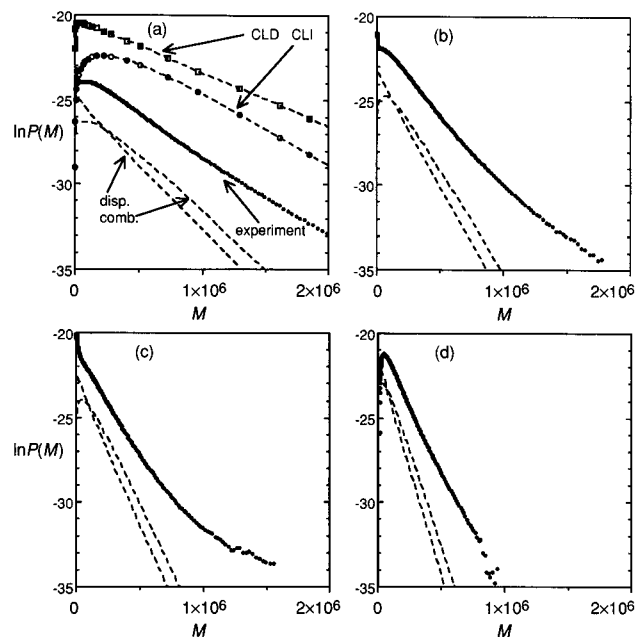


Figure 10. Simulated (lines) and experimental (points) $\ln P(M)$ at (a) 5.35×10^{-3} , (b) 1.60×10^{-2} , (c) 2.67×10^{-2} , and (d) $5.35 \times 10^{-2} \text{ mol dm}^{-3}$ AIBN in set PCLC2 (styrene). "comb." and "disp." simulated MWDs are for all termination by disproportionation (concave up at low M) and for all termination by combination (concave down at low M), "CLI" and "CLD" are for all termination by combination and with chain-length-independent and -dependent parameters; parameter values as in text. All simulations are for 2.0% conversion; simulated curves are displaced along the ordinate for clarity. Experimental instantaneous conversions are those from Figure 6 which are closest to 2%.

upturn in $\ln P(M)$ in Figure 10 cannot be as readily explained. This portion of the MWD is at molecular weights for which no polymer could be detected in the equivalent MMA experiments. This suggests firstly that this upturn may be a result of column broadening. If column broadening is operative only below a molecular weight of 2×10^4 , it would not be observable in $\ln P(M)$ for poly(MMA), because no polymer of such low M was detectable. A second possibility is that the GPC calibration curve was slightly in error for M less than 2×10^4 ; a third possibility is adventitious chain-transfer agent (see above). All things considered, it appears that the upturn in $\ln P(M)$ for polystyrene is an artifact.

Some simulated $\ln P(M)$ are also given in Figure 10, for which $x = 0.02$ was used; for clarity, all simulated $\ln P(M)$ have been displaced by an arbitrary amount on the ordinate (recall the normalization of $P(M)$ is arbitrary). The parameter values were those discussed above ($k_t^0 = 10^8 \text{ dm}^3 \text{ mol}^{-1} \text{ s}^{-1}$, large σ , etc.). The simulated curves denoted "comb." and "disp." denote all termination by combination and disproportionation, respectively; for clarity, the labeling is only given in Figure 10a. With parameter values chosen to give accord with the experimental high- M slope, the computed $\ln P(M)$ are sensitive to the value of k_{tr} , showing that transfer to monomer is a significant chain-stopping event.

(i) The curves denoted "CLI" and "CLD" in Figure 10a were calculated with parameter values chosen to approximately match the high- M part of the experimental $\ln P(M)$. CLD is for the strongest chain-length dependence: calculated with the "expected" parameter values discussed in section 2.1, including $k_t^0 = \infty$. "CLI" is the chain-length-independent result, which has no

further parameters after this choice, since its functional form is $P(M) = M \exp(-2M/(M_n))$; it will be recalled that comparison of this CLI curve with experiment is important because it refutes the assumption of total chain-length independence for chain stoppage in this styrene system, since this chain-length independence would give a maximum which is not observed experimentally if the curve is also constrained to give accord with the experimental high- M part of $\ln P(M)$. (ii) The simulations with termination by disproportionation show something of the low- M upturn in $\ln P(M)$ that is shown by the experiments. However, the experimental upturn is always much sharper than that of the simulations, so it may be considered unlikely that this upturn evidences termination by disproportionation and may well be due to adventitious chain-transfer agent. (iii) On the basis of the rest of the experimental $\ln P(M)$ alone (i.e., the portions beyond the low- M upturns), it is impossible to make any conclusions regarding the mode of termination, for over these regions there are no significant shape differences between the two types of simulation results. Thus, our experimental MWDs are not inconsistent with the well-established result that styrene termination is predominantly by combination.^{52,53}

5. Summary and Conclusions

The aim of this work was to examine the rate and molecular weight distribution of bulk polymerizations of both styrene and MMA at low conversion, by comparing experiment and the predictions of a comprehensive, microscopic theory. The specific variables which were examined were the rate of polymerization, the long-chain slope of $\ln P(M)$ (denoted Λ), and the shape of the low- M portion of the full number molecular weight distribution.

The most important result is the experimental verification of the prediction that MWDs, when plotted as $\ln(\text{number distribution})$, should show extensive linear regions if chain stoppage is dominated by transfer and/or disproportionation (MMA) and/or chain-length-dependent combination (styrene). While moderate agreement was obtained between the predicted and experimental Λ values if termination was always assumed to be chain-length dependent ($k_t^0 = \infty$), this predicts (in contradiction to experiment) that R_p increases, and Λ decreases, with conversion. Putting $k_t^0 = \infty$ also does not give adequate accord for the variations of R_p and Λ with initiator concentration. In all cases except for the dependence of Λ_{exp} upon initiator concentration for MMA, either a weaker dependence of termination rate coefficients upon chain length or a higher k_{tr} is needed to predict the dependences of experimental R_p and Λ_{exp} upon $[I]$. Some of these discrepancies can be overcome by assuming that there is a large chain-length-independent component for k_t . Accord with experimental rates and MWDs for styrene could be obtained by assuming that there is a significant chain-length-independent component to chain stoppage, as well as a significant chain-length dependent one, the latter with an interaction distance much greater than that of a monomer unit. A number of postulates can be made on the complexities in the dynamics of termination, such as the ends of chains sweeping out a volume larger than that covered by center-of-mass diffusion (i.e., a value of the interaction distance σ larger than that of a monomer unit).

The present low-conversion data are most consistent with termination containing a significant chain-length-

independent component. This is in marked contrast to corresponding data for styrene at *intermediate* and *high* conversion,¹¹ which show conclusively that termination is chain-length dependent. This can be readily understood in terms of slower diffusion at higher conversions, changing the rate-determining step.

Attempts to see if our MWDs could give information on the mode of termination were unfruitful, because the shapes of combination-dominated and disproportionation-dominated $\ln P(M)$ are significantly different only at such low M that the GPC data are subject to too great uncertainty.

Overall, the model used in this paper provides a reasonable but imperfect description of the kinetics and MWD of the low-conversion bulk polymerizations of styrene and MMA.

Acknowledgment. The support of the Australian Research Council is gratefully acknowledged, as is that of an Australian Postgraduate Research Award for P.A.C. We also greatly appreciate the assistance of Ms. Jelica Hutovic with some of the experimental work described in this paper, as well as the assistance of Rodd Snook and Stuart Prescott in diagram and manuscript preparation and helpful comments on the manuscript by David Sangster.

References and Notes

- (1) Clay, P. A.; Gilbert, R. G. *Macromolecules* **1995**, *28*, 552.
- (2) Allen, P. E. M.; Patrick, C. R. *Makromol. Chem.* **1961**, *47*, 154.
- (3) Benson, S. W.; North, A. M. *J. Am. Chem. Soc.* **1962**, *84*, 935.
- (4) Scheren, P. A. G. M.; Russell, G. T.; Sangster, D. F.; Gilbert, R. G.; Gorman, A. L. *Macromolecules* **1995**, *28*, 3637.
- (5) Russell, G. T. *Macromol. Theory Simul.* **1995**, *4*, 497.
- (6) Russell, G. T. *Macromol. Theory Simul.* **1995**, *4*, 519.
- (7) Russell, G. T. *Macromol. Theory Simul.* **1995**, *4*, 549.
- (8) Russell, G. T.; Gilbert, R. G.; Napper, D. H. *Macromolecules* **1993**, *26*, 3538.
- (9) Russell, G. T.; Gilbert, R. G.; Napper, D. H. *Macromolecules* **1992**, *25*, 2459.
- (10) Cunningham, B. F.; Mahabadi, H. K. *Macromolecules* **1996**, *29*, 835.
- (11) Clay, P. A.; Christie, D. I.; Gilbert, R. G. *Polym. Prepr.*, in press.
- (12) Schulz, G. V. *Z. Phys. Chem. (Frankfurt am Main)* **1956**, *8*, 290.
- (13) Gilbert, R. G. *Emulsion Polymerization: A Mechanistic Approach*; Academic: London, 1995.
- (14) Mahabadi, H. K.; O'Driscoll, K. F. *J. Polym. Sci., Part A: Polym. Chem.* **1977**, *15*, 283.
- (15) Mahabadi, H. K.; O'Driscoll, K. F. *Macromolecules* **1977**, *10*, 55.
- (16) Hutchinson, R. A.; Aronson, M. T.; Richards, J. R. *Macromolecules* **1993**, *26*, 6410.
- (17) Gilbert, R. G. *Pure Appl. Chem.* **1996**, *68*, 1491.
- (18) Buback, M.; Garcia-Rubio, L. H.; Gilbert, R. G.; Napper, D. H.; Guillot, J.; Hamielec, A. E.; Hill, D.; O'Driscoll, K. F.; Olaj, O. F.; Shen, J.; Solomon, D.; Moad, G.; Stickler, M.; Tirrell, M.; Winnik, M. A. *J. Polym. Sci., Polym. Lett. Ed.* **1988**, *26*, 293.
- (19) Buback, M.; Gilbert, R. G.; Hutchinson, R. A.; Klumperman, B.; Kuchta, F.-D.; Manders, B. G.; O'Driscoll, K. F.; Russell, G. T.; Schweer, J. *Macromol. Chem. Phys.* **1995**, *196*, 3267.
- (20) Heuts, J. P. A.; Radom, L.; Gilbert, R. G. *Macromolecules* **1995**, *28*, 8771.
- (21) Morrison, B. R.; Casey, B. S.; Lacik, I.; Leslie, G. L.; Sangster, D. F.; Gilbert, R. G.; Napper, D. H. *J. Polym. Sci. A: Polym. Chem.* **1994**, *32*, 631.
- (22) Tobolsky, A. V.; Offenbach, J. *J. Polym. Sci.* **1955**, *16*, 311.
- (23) Whang, B. C. Y.; Ballard, M. J.; Napper, D. H.; Gilbert, R. G. *Aust. J. Chem.* **1991**, *44*, 1133.
- (24) Brandrup, A.; Immergut, E. H. In *Polymer Handbook*; 3rd ed.; Brandrup, A., Immergut, E. H., Eds.; Wiley Interscience: New York, 1989.
- (25) Stickler, M. *Makromol. Chem.* **1982**, *184*, 2563.
- (26) Fischer, H.; Henning, P. *Acc. Chem. Res.* **1987**, *20*, 200.

- (27) Stukelj, M.; Martinho, J. M. G.; Winnik, M. A.; Quirk, R. P. *Macromolecules* **1991**, *24*, 2488.
- (28) Reid, R. C.; Sherwood, T. K. *The Properties of Gases and Liquids*; 2nd ed.; McGraw-Hill: New York, 1966.
- (29) Griffiths, M. C.; Gilbert, R. G. To be published.
- (30) Piton, M. C.; Gilbert, R. G.; Chapman, B. E.; Kuchel, P. W. *Macromolecules* **1993**, *26*, 4472.
- (31) Lee, J. A.; Frick, T. S.; Huang, W. J.; Lodge, T. P.; Tirrell, M. *Polym. Prepr.* **1987**, *28*, 369.
- (32) Pickup, S.; Blum, F. D. *Macromolecules* **1989**, *22*, 3961.
- (33) Kosfeld, R.; Goffloo, K. *Kolloid-Z. Z. Polym.* **1971**, *247*, 801.
- (34) Goffloo, K.; Kosfeld, R. *Angew. Makromol. Chem.* **1974**, *37*, 105.
- (35) Landry, M. R.; Gu, Q. *Macromolecules* **1988**, *21*, 1158.
- (36) Faldi, A.; Tirrell, M.; Lodge, T. P.; von Meerwall, E. D. *Polym. Prepr.* **1991**, *32*, 400.
- (37) Russell, G. T.; Napper, D. H.; Gilbert, R. G. *Macromolecules* **1988**, *21*, 2133.
- (38) Ballard, M. J.; Gilbert, R. G.; Napper, D. H.; Pomery, P. J.; O'Donnell, J. H. *Macromolecules* **1984**, *17*, 504.
- (39) Leest, Y.; Smets, G. *J. Polym. Sci., Polym. Chem. Ed.* **1988**, *26*, 913.
- (40) Berens, A. R.; Hopfenberg, H. B. *J. Memb. Sci.* **1982**, *10*, 283.
- (41) Kosfeld, R.; Schlegel, J. *Angew. Makromol. Chem.* **1973**, *29/30*, 105.
- (42) Balke, S. T.; Hamielec, A. E. *J. Appl. Polym. Sci.* **1973**, *17*, 905.
- (43) Olaj, O. F.; Zifferer, G.; Gleixner, G. *Macromolecules* **1987**, *20*, 839.
- (44) Mahabadi, H. K. *Macromolecules* **1985**, *18*, 1319.
- (45) Mahabadi, H. K. *Macromolecules* **1991**, *24*, 606.
- (46) Gallot-Grubisic, Z.; Rempp, P.; Benoit, H. *Polym. Lett.* **1967**, *5*, 753.
- (47) Shortt, D. W. *J. Liquid Chromatogr.* **1993**, *16*, 3371.
- (48) Stickler, M. *Makromol. Chem.* **1979**, *180*, 2615.
- (49) Olaj, O. F.; Zifferer, G. *Macromolecules* **1987**, *20*, 850.
- (50) Yamada, B.; Yoshikawa, E.; Miura, H.; Otsu, K. *Makromol. Chem., Rapid Commun.* **1992**, *13*, 531.
- (51) Bowry, V. W.; Ingold, K. U. *J. Am. Chem. Soc.* **1992**, *114*, 4992.
- (52) Moad, G.; Solomon, D. H. In *Comprehensive Polymer Science*; Eastmond, G. C., Ledwith, A., Russo, S., Sigwalt, P., Eds.; Pergamon: London, 1989; Vol. 3, p 147.
- (53) Moad, G.; Solomon, D. H. *The Chemistry of Free Radical Polymerization*; Pergamon: Oxford, 1995.
- (54) Zammit, M. D.; Davis, T. P.; Haddleton, D. M. *Macromolecules* **1996**, *29*, 492.
- (55) Ito, Y.; Tsuge, S.; Ohtani, H.; Wakabayashi, S.; Atarashi, J.; Kawamura, T. *Macromolecules* **1996**, *29*, 4516.
- (56) Mahabadi, H. K.; Rudin, A. *J. Polym. Sci., Part A: Polym. Chem.* **1979**, *17*, 1801.
- (57) North, A. M.; Reed, G. A. *Trans. Faraday Soc.* **1961**, *57*, 859.
- (58) Cardenas, J. N.; O'Driscoll, K. F. *J. Polym. Sci., Polym. Chem. Ed* **1979**, *17*, 1891.
- (59) Kent, M. S.; Faldi, A.; Tirrell, M.; Lodge, T. P. *Macromolecules* **1992**, *25*, 4501.
- (60) Arai, T.; Abe, F.; Yoshizaki, T.; Einaga, Y.; Yamakawa, H. *Macromolecules* **1995**, *28*, 3609.
- (61) Olaj, O. F.; Kauffmann, H. F.; Breitenbach, J. W. *Makromol. Chem.* **1977**, *178*, 2707.
- (62) Stickler, M.; Meyerhoff, G. *Makromol. Chem.* **1978**, *179*, 2729.

MA960367H